Tracking Oxytetracyline Mobility Across Environmental Interfaces by Second Harmonic Generation

Amanda L. Mifflin, Christopher T. Konek, and Franz M. Geiger*

Department of Chemistry, Northwestern University, 2145 Sheridan Road, Evanston, Illinois 60208
Received: May 19, 2006; In Final Form: September 5, 2006

This work examines the binding behavior of the antibiotic oxytetracycline (OTC) to mineral oxide/water interfaces in the presence and absence of organic functional groups using the interface-specific technique second harmonic generation (SHG). Studies show that OTC binding to fused quartz, methyl ester, carboxylic acid, and alkyl interfaces is fully reversible and highly dependent on solution pH, with appreciable adsorption occurring only at pH 8. Relative surface coverage at pH 8 is highest for the polar organic-functionalized surfaces, and surface saturation occurs for the methyl ester-functionalized fused quartz/water interface at 2×10^{-5} M. Adsorption isotherm measurements indicate that the binding process is controlled by hydrogen bonding and hydrophobic interactions, with free energies of adsorption on the order of −40 kJ/mol for all interfaces studied. The results indicate that OTC transport in the environment will depend heavily on soil pH and composition and have implications for the development of bacterial antibiotic resistance.

1. Introduction

A. Agricultural Pharmaceuticals and Antibiotic Resistance. The detection of low levels of veterinary and human antibiotics in ground and surface waters has raised concerns over the fate of such compounds once they are introduced into the environment.[1−17] The agricultural nontherapeutic use of antibiotics can stimulate growth in farm animals.[4,5,18−21] However, the use of antibiotics in this manner, especially those that are closely related in functionality to human-use antibiotics, can have a significant impact on antibiotic effectiveness in humans.[18−28] In general, the development of drug resistance in microorganisms has made it significantly more difficult to treat infections of disease-causing bacteria that once were relatively easy to treat, including *Salmonella* and *E. coli*.[29] Most notably, the death of a woman in 1998 from a drug-resistant strain of *Salmonella* was directly linked to antibiotic use on a swine farm in Denmark.[22] In addition, direct exposure to concentrations of pharmaceuticals in the ng/L range detected in a number of rivers in the United States has caused concern about their presence in municipal water systems.[7] However, the low concentration of pharmaceuticals reported in these studies is generally not nearly as high a concern for human health as compared to that posed by the emerging threat of bacterial antibiotic resistance due to the agricultural use of pharmaceuticals. The latter issue has gained increased governmental attention in recent years. For instance, in the United States, an Interagency Task Force on Antimicrobial Resistance was created in 1999 and includes, among others, the Centers for Disease Control and Prevention, the Food and Drug Administration (FDA), the Department of Agriculture, and the Environmental Protection Agency.[30] Recently, the FDA banned the use of the veterinary antibiotic Baytril, which is used on poultry farms, because it is chemically very similar to ciprofloxacin, which is used in humans to combat bacterial infections, including anthrax.[31] On a global scale, the World Health Organization released a report in 2000 addressing the human health concerns of antimicrobial drug resistance[32] and has called for the elimination of nontherapeutic antibiotic use in the livestock industry.[19] Endorsed by the American Medical Association, legislative action has also been proposed to the U.S. Congress that would prevent farmers from using human antibiotics for nontherapeutic purposes unless proven safe for human health.[19]

B. Drug Mobility in Soils: Linking Antibiotic Resistance with Agricultural Pharmaceuticals. Some antibiotics administered to farm animals are excreted 50−80% unmetabolized,[2,33] resulting in antibiotic-laced manure that can be introduced into the environment via mechanisms that can include farm runoff and use of manure in fertilizer formulations. Although the relationship between antibiotic use on farms and antibiotic resistance in bacteria has been confirmed,[34−37] there is little information available concerning the transport of antibiotics in soil environments and its link to bacterial antibiotic resistance. Assessing the mobility of antibiotics in soils is of particular interest as a means to determine (1) if an antibiotic is expected to display a high contact frequency with bacteria in soils and (2) if the antibiotic is likely to enter the groundwater, where it can be transported over large distances. Specifically, highly mobile antibiotics can move easily through the soil, where bacteria will be exposed to the drug, resulting in drug-resistance and in drug-resistance transfer to other bacterial species through quorum sensing,[38,39] further increasing the range of exposure.[22,40] In addition, highly mobile drugs are more likely to impact neighboring areas, with a potential for exposure of farms that do not use antibiotics to drugs from nearby farms that use antibiotics via groundwater transport or runoff from precipitation events.

In soils, mineral oxide/water interfaces can play a crucial role in controlling contaminant transport in the environment.[41−43] Interface-specific investigations of the interactions between antibiotics and mineral surfaces are therefore necessary to gain a molecular-level understanding of antibiotic mobility in the environment and its potential to increase antibiotic resistance due to highly mobile antibiotics used in agriculture.

C. Oxytetracycline. In this laboratory study, we apply a nondestructive, submonolayer-sensitive optical probe that is

* To whom correspondence should be addressed. E-mail: geigerf@chem.northwestern.edu.

10.1021/jp063089p CCC: $33.50
Published on Web 10/17/2006

specific to mineral/water interfaces to track the interaction of the human and veterinary antibiotic oxytetracycline (OTC) with fused quartz/water interfaces in the presence and absence of organic adlayers. Similar to our previous work that assessed the mobility of hexavalent chromium[44−47] and that of the veterinary antibiotic morantel[48] across mineral/water interfaces, the experiments are carried out using resonance-enhanced surface second harmonic generation (RES-SHG) and employ fused quartz as the solid substrate because silicon oxides are ubiquitous in soil minerals. The organic adlayers are formed by linking environmentally important organic functional groups, namely carboxylic acid, ester, and alkyl groups, to the fused quartz surface via silane chemistry.[49]

Oxytetracycline was discovered in the soil microorganism *aureofaciens* by Benjamin Minge Duggar in 1947.[50] In 1955, it was patented under the name terramycin to Lloyd Conover, who chemically altered the naturally produced drug into a more stable form by catalytic hydrogenation.[50−53] Woodward and Conover then determined the chemical structure of the antibiotic using UV−vis spectroscopy.[50] Oxytetracycline is a member of the tetracycline family of antibiotics. Tetracyclines are important for treating bacterial illnesses such as acne, bronchitis, and lyme disease,[50,54] but use of tetracyclines in humans extends beyond their antibiotic function. They have been frequently used to treat rheumatoid arthritis because of their anti-inflammatory properties and also to treat periodontal disease as an inhibitor of connective tissue breakdown.[50] Oxytetracycline acts as an antibiotic by interfering with the binding of the aminoacyl-tRNA-EF-Tu-GTP ternary complex to ribosomal DNA, which affects the bacteria's ability to produce proteins.[50,54] It is active against a wide range of bacteria, including Gram-negative and Gram-positive bacteria, rickettsiae, and protozoan parasites.[50,54] Tetracyclines, once the most prescribed broad-spectrum antibiotics, are also among the most widely used nontherapeutic feed additives in the United States. In 2000, 250 000 pounds of tetracycline were used for human therapy in the United States,[13] whereas 3 million pounds are used yearly for agricultural purposes as a nontherapeutic feed additive for growth stimulation.[11] OTC has been detected in surface-water measurements at concentrations up to 72 μg/L.[3,55] Although human exposure to this low concentration of OTC is not considered to be a large risk, there is concern about the fate of OTC in the environment and its potential for contributing to bacterial antibiotic resistance.[55] Data also suggests that OTC is persistent in anoxic soils, with an estimated half-life of 10 weeks.[2]

Evidence of bacterial antibiotic resistance has been reported for soils exposed to oxytetracycline-treated swine manure.[55] This is not surprising, as resistance to oxytetracycline was documented only a few years after its introduction as a commercial antibiotic,[28,56] and its usefulness in treating illnesses has diminished significantly in recent years.[54,57] Resistance to tetracyclines is currently believed to occur through three possible pathways: (1) tetracycline efflux, which lowers the concentration of tetracycline in the cell, (2) production of ribosomal protection proteins, and (3) enzymatic inactivation of tetracycline.[50,54] Interestingly, the nontherapeutic use of tetracycline was banned by the United Kingdom in the early 1970s, whereas its agricultural use continues in the United States.[29]

At environmentally relevant pH values, the molecule can exist as the cation (OTC^{+00}), the zwitterion (OTC^{+-0}), and the monoanion (OTC^{+--}) in bulk aqueous solution, with corresponding pK_a values of 3.27, 7.32, and 9.11, respectively (Figure 1).[6,10−12,33,58−60] This complex solution chemistry can have a significant impact on oxytetracycline sorption behavior with environmental surfaces. Many studies have been conducted that examine OTC spectroscopy and sorption behavior[2,3,6,10−12,33,58,59,61] and indicate that OTC sorption is influenced by soil texture, cation exchange capacity, soil pH, soil clay content, and iron oxide content. Specifically, OTC has been shown to sorb strongly to clays in acidic environments.[33,59] Sorption is also significant in iron and aluminum-oxide-rich soils in more alkaline environments,[62,63] and ternary complex formation between OTC, metal cations, and organic matter ligands appears to facilitate sorption to soil surfaces.[64] Additionally, a study by Kulshrestha et al. suggests that OTC sorption in alkaline soils is dominated by hydrophobic interactions rather than cationic exchange.[12] These studies utilize primarily X-ray and batch techniques, which are powerful tools for assessing OTC sorption and relative transport through soil and clays. However, these techniques have some limitations in sensitivity and the elucidation of molecular-level binding mechanisms. In this work, we use a model for silica-rich, nonclay soil environments that can be functionalized with organic groups common in natural organic matter. SHG studies allow us to access surface-specific thermodynamic binding parameters at environmentally relevant concentrations that can be used to develop improved transport models for oxytetracycline in the environment.

2. Experimental Section

The oxytetracycline hydrochloride (VWR) absorbance spectra exhibit strong electronic transitions at approximately 275 and 355 nm for the pH range 4−9. These peaks shift for acidic (270 and 355 nm) or basic (265 and 375 nm) solutions (Figure 1). The peak at 275 nm is due to the A chromophore, comprised of the tricarbonyl system.[50,65,66] The peak at 355 nm has been assigned to the BCD chromophore that encompasses the π-system of the phenolic diketone group (Figure 1).[65] This electronic signature makes oxytetracycline an ideal candidate for study by second harmonic generation.

The measured second harmonic signal intensity, I_{SHG}, is related to the second-order susceptibility of the interface, $\vec{\vec{\chi}}^{(2)}$, which has both resonance (R) and nonresonance (NR) contributions[67−69]

$$\sqrt{I_{SHG}} \propto \vec{\vec{\chi}}_R^{(2)} + \vec{\vec{\chi}}_{NR}^{(2)} \tag{1}$$

In the case of resonance-enhanced SHG, the resonance second-order susceptibility can be modeled by[67−69]

$$\vec{\vec{\chi}}_R^{(2)} = N_{ads}\langle\vec{\vec{\alpha}}^{(2)}\rangle \tag{2}$$

where N_{ads} is the number of adsorbed species at the interface and $\langle\vec{\vec{\alpha}}^{(2)}\rangle$ is the molecular hyperpolarizability averaged over all molecular orientations. Thus, by monitoring the square root of the SHG intensity, one can obtain information about relative adsorbate surface coverage. The $\langle\vec{\vec{\alpha}}^{(2)}\rangle$ term is described by the summation over excited states of factors that are related to the electronic transitions of the adsorbed species[67−69]

$$\langle\vec{\vec{\alpha}}^{(2)}\rangle = -\frac{4\pi^2 e^3}{\hbar^2} \times \sum_{b,c}\left[\frac{\langle a|\vec{\mu}_i|b\rangle\langle b|\vec{\mu}_j|c\rangle\langle c|\vec{\mu}_k|a\rangle}{(\omega_{ba} - \omega - i\Gamma_{ba})(\omega_{ca} - 2\omega - i\Gamma_{ca})} + ...\right] \tag{3}$$

where e is the charge of an electron, $\hbar$ is Planck's constant, $\vec{\mu}_i$ is the electric dipole moment operator, and a, b, and c represent the ground, intermediate, and final states, respectively. Equation

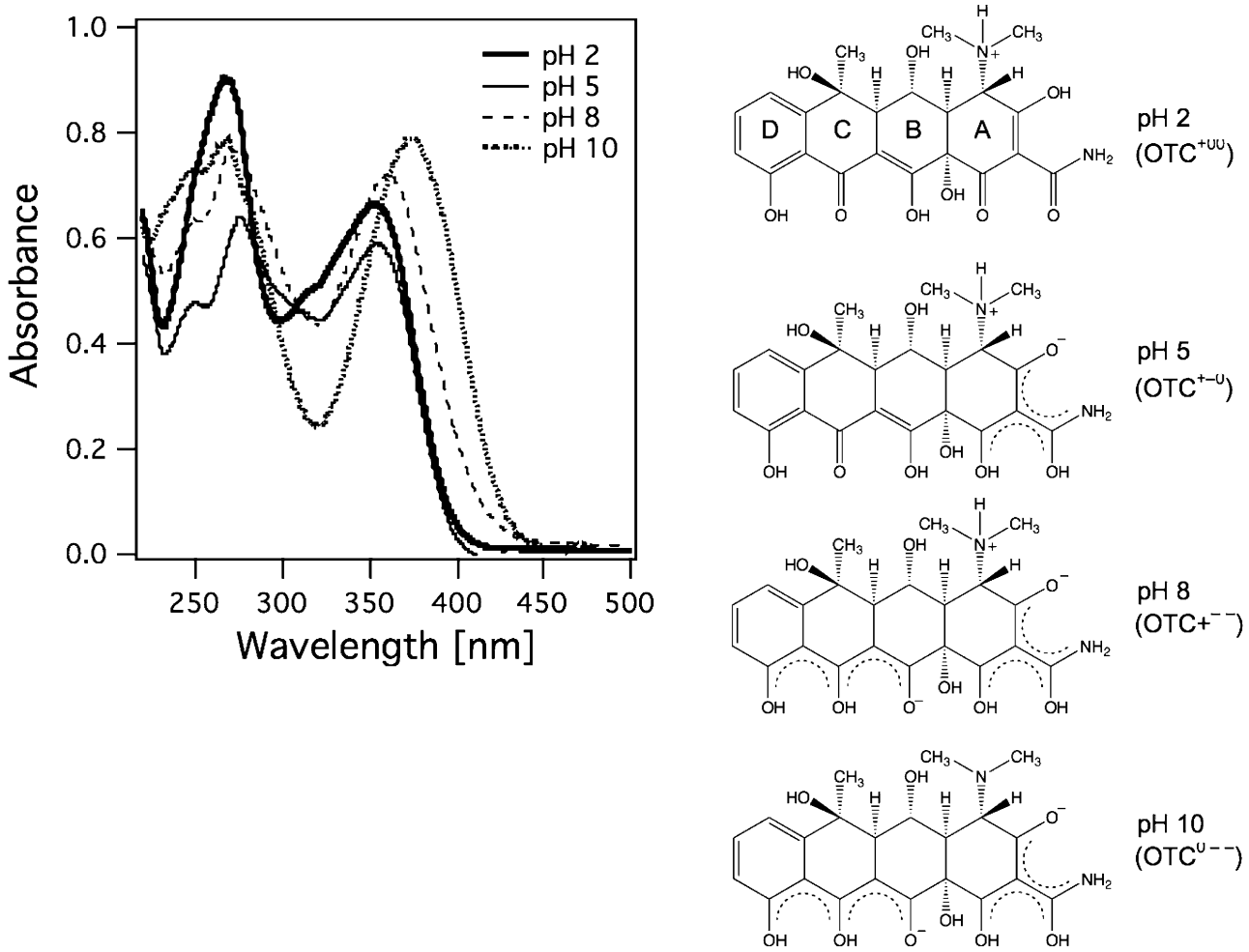

Figure 1. Bulk UV−vis spectra for 5×10^{-5} M aqueous oxytetracycline HCl at pH 2, 5, 8, and 10. The spectra correspond to the different protonation states of the OTC molecule in solution. Structures of the four species are depicted at the right.

3 shows that as the fundamental frequency, ω, or the second harmonic frequency, 2ω, approach natural resonance frequencies of the adsorbed species, ω_{ba} or ω_{ca}, the hyperpolarizability increases, corresponding to an enhancement of the SHG signal intensity. This condition allows one to obtain spectroscopic information for the interface in the UV−vis spectral region.

The SHG studies were carried out using a regeneratively amplified Ti:Sapphire laser system (Hurricane, Spectra Physics) pumping an optical parametric amplifier (OPA-CF, Spectra Physics). The optical setup has been described in detail previously.[44,45] The visible output beam from the OPA at frequency ω was directed onto the interface, and the second harmonic signal at 2ω was detected using a monochromator and gated photon counting system. The fundamental light was filtered out using Schott filters.

The mineral oxide/water interface was created using a fused quartz hemispherical lens (ISP Optics) placed atop a custom-built Teflon flow cell and held leak-tight using a Viton O-ring. Millipore water and oxytetracycline hydrochloride (VWR) solutions were pumped across the interface using variable flow peristaltic pumps, allowing for full control over the flow rates of both solutions. The solution pH was adjusted using standard NaOH and HCl solutions (Fisher). Experimental details of the flow cell system have been published.[44,45]

The stock solutions used to prepare standard dilutions required pH adjustment after addition of the acidic salt. Because of the difficulty in monitoring the solution pH in volumetric flasks, the stock solutions were prepared in beakers. For each stock solution, the mass of oxytetracycline was weighed directly on a balance, and approximately 50 g of Millipore water was added to dissolve the salt. NaOH or HCl solution was then added to bring the solution to the desired pH. Millipore water at the same pH was then added to bring the solution mass to 100 g. Once the oxytetracycline was dissolved in aqueous solution and adjusted to the desired pH, the pH remained stable for subsequent dilutions with Millipore water, allowing dilutions to be conducted with volumetric flasks. This procedure resulted in oxytetracycline concentrations in units of molality. However, at concentrations below 0.01 mol/L,[70] the oxytetracycline molalities used in this work (all below 4×10^{-4} M) can be expressed in terms of molarity. Calibration curves were measured for each pH, resulting in molar extinction coefficients of $1.46(3) \times 10^4$ cm^{-1} M^{-1} for pH 2 at $\lambda_{max} = 355$ nm, $1.30(2) \times 10^4$ cm^{-1} M^{-1} for pH 5 at $\lambda_{max} = 355$ nm, $1.57(3) \times 10^4$ cm^{-1} M^{-1} for pH 8 at $\lambda_{max} = 360$ nm, and $1.74(2) \times 10^4$ cm^{-1} M^{-1} for pH 10 at $\lambda_{max} = 375$ nm.

III. Results and Discussion

A. SHG Surface Spectroscopy. The SHG spectrum of oxytetracycline adsorbed to the fused quartz/water interface was recorded at pH values of 2, 5, 8, and 10, which correspond to the cation, neutral, monoanion, and dianion species of OTC in solution. The spectra were collected by monitoring the SHG signal of a fused quartz/water interface in contact with a 50 μM aqueous solution of OTC as a function of incident fundamental wavelength with a constant energy of 2 μJ/pulse.

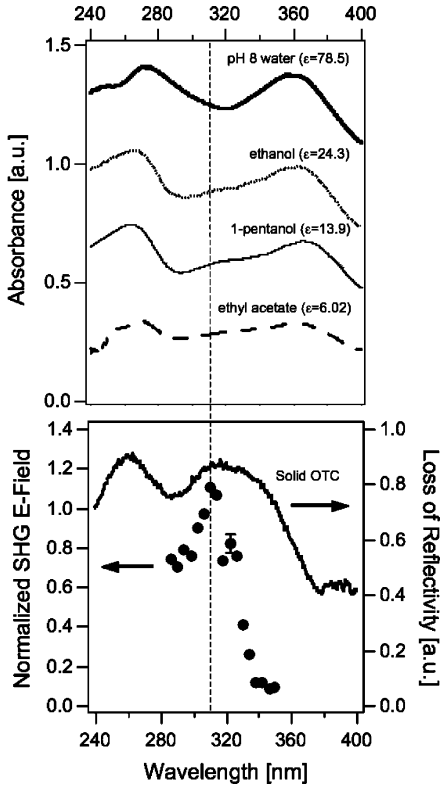

Figure 2. Top panel shows bulk UV−vis spectra for oxytetracycline HCl dissolved in solvents with varying dielectric constants, increasing from bottom to top. Dashed line, ethyl acetate ($\epsilon = 6.02$); thin solid line, 1-pentanol ($\epsilon = 13.9$); dotted line, ethanol ($\epsilon = 24.3$); thick solid line, water at pH 8 ($\epsilon = 78.5$). Spectra are offset for clarity. Bottom panel shows a solid-state reflection UV−vis spectrum (solid line). The loss of reflectivity is calculated from the absolute value of the difference between the OTC reflection spectrum and a KBr reference. Filled circles are the SHG spectrum of OTC at the silica/water interface at pH 8 and 5×10^{-5} M.

The most pronounced signal increase occurs at pH 8 at 307 nm, shown by the black circles in Figure 2. The SHG spectrum for OTC, however, does not appear to match the respective bulk spectrum at pH 8, which shows peaks at approximately 275 and 360 nm (top trace in Figure 2). This is possibly due to blue shifting of the OTC aqueous phase spectrum upon adsorption to the interface, which has been shown to occur in hydrogen bonding interactions of $n-\pi^*$ systems induced by small changes in the bond lengths of the ground and excited states.[71] This effect has been shown in computational studies to be most significant for proton acceptors at moderately basic pH.[72] In this case, the detected SHG resonance centered around 307 nm would be due to a blue-shifted BCD transition. At the silica/water interface and neutral pH, a similar blue-shifted SHG resonance enhancement has been observed for the case of hexavalent chromium, CrO_4^{2-}, which also exhibits acid−base behavior, but not for morantel, which does not undergo protonation or deprotonation.[48]

However, the SHG resonance enhancement at 307 nm is also consistent with a shoulder on the BCD chromophore transition in the OTC aqueous bulk spectra at pH 2, 5, and 8 (Figure 1). To the best of our knowledge, this shoulder has not been spectroscopically assigned in the literature. Figure 2 shows that this shoulder becomes more pronounced in organic solvents with lower dielectric constants. Finally, the solid-state OTC spectrum, which was collected by detecting the reflection from the surface of a pressed pellet of OTC in a KBr matrix using a UV−vis spectrometer, shows a high absorbance at the wavelength at which SHG resonance enhancement of OTC at the fused quartz/water interface is highest. This result suggests that the chromophore that is involved in the SHG resonance enhancement may be in a low-dielectric environment. This is consistent with the notion that solvent water molecules surround only a portion of OTC when it is adsorbed at the liquid/solid interface.

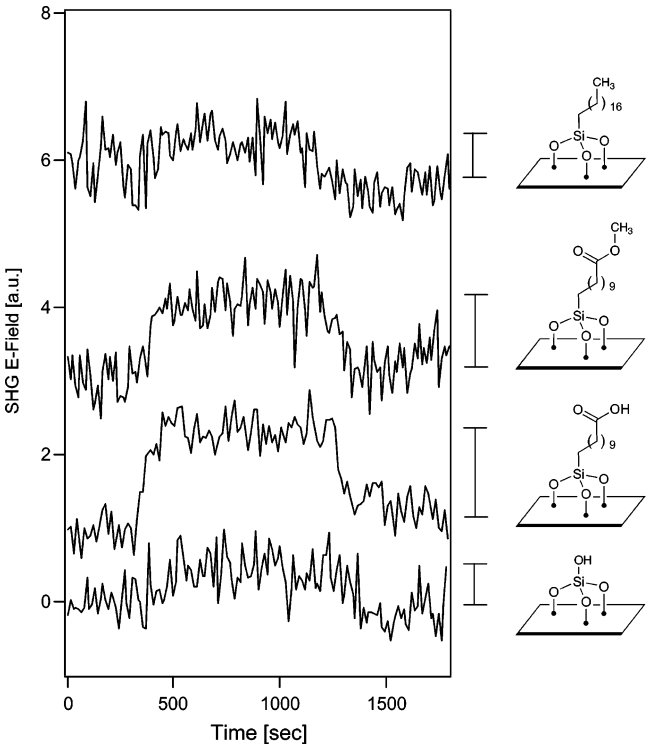

Figure 3. Representative OTC adsorption/desorption traces for (from bottom) fused quartz/water, carboxylic acid-functionalized fused quartz/water, methyl ester-functionalized fused quartz/water, and octadecyl alkane-functionalized fused quartz/water interfaces recorded at pH 8 and 1×10^{-5} M. Traces offset for clarity.

B. Adsorption/Desorption Traces. OTC adsorption/desorption experiments were conducted by exposing the fused quartz/water interface in the presence and absence of organic adlayers at pH 2, 5, 8, and 10 to 1×10^{-5} M aqueous solutions of oxytetracycline. Four interfaces were investigated: the plain fused quartz/water interface, a methyl ester-functionalized fused quartz/water interface, and fused quartz/water interfaces functionalized with carboxylic acid groups and an octadecyl alkane. Preparation and characterization of these surfaces were carried out using silane chemistry, SHG, and vibrational sum frequency generation (SFG) and have been described previously.[73−77] A longer carbon chain was chosen for the alkyl-terminated adlayer in order to facilitate packing of the adlayer. The experiment begins with a 5 min baseline collection, where the substrate is exposed to water at a given pH, followed by a 15 min adsorption and equilibration period, in which the interface is in contact with OTC at a given concentration and the same pH, and ends with a 10 min desorption period, in which the OTC solution above the interface is replaced by water at the same pH.

The results for pH 8 are shown in Figure 3. According to eq 2, the square root of the SHG signal intensity is proportional to the number density, or surface coverage, of OTC. Clearly, Figure 3 shows that OTC does adsorb to all four interfaces, as evidenced by the SHG E-field increase. The adsorption and desorption processes for all interfaces examined are fully reversible and complete within five minutes of turning the OTC flow on and off, respectively. At pH 8, it appears that the extent of adsorption is highest for the polar organic methyl ester and

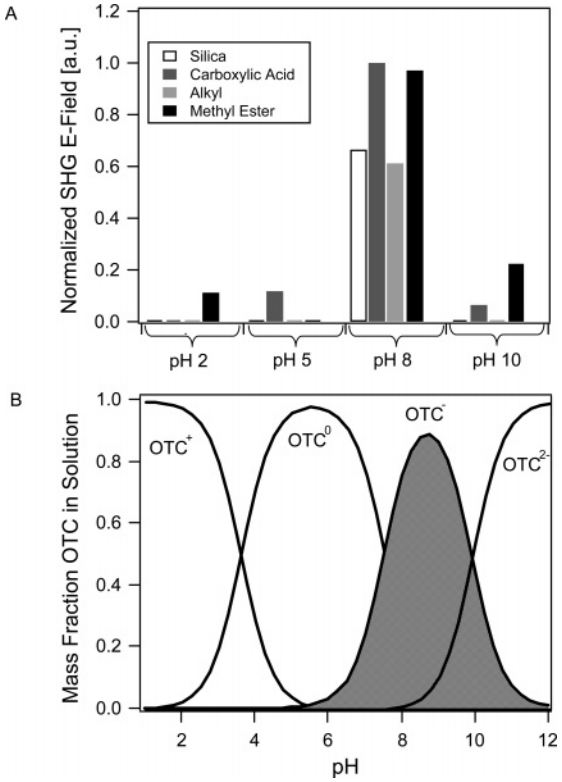

Figure 4. (A) Normalized SHG signal increase for monolayer concentrations of OTC adsorbed to the interfaces investigated at pH 2, 5, 8, and 10. White bars, fused quartz/water; dark gray bars, carboxylic acid-functionalized fused quartz/water; light gray bars, octadecyl alkane-functionalized fused quartz/water; black bars, methyl ester-functionalized fused quartz/water. Data calculated from adsorption isotherm measurements. (B) Plot of OTC speciation as a function of bulk solution pH. OTC binding to interfaces under investigation is most significant when in the monoanion form (shaded region).

carboxylic acid adlayers. This result indicates that the combination of carbonyl and alkyl groups enhances the interaction of oxytetracycline with the interface. This suggests that a combination of hydrogen bonding and hydrophobic interactions facilitates binding. The presence of long alkyl chains below the carboxylic acid and ester groups at the interface may provide OTC with an opportunity for insertion into the hydrophobic portion of the adlayers, resulting in increased surface coverage. In contrast, the surfaces that only undergo one type of interaction (H-bonding in the case of the fused quartz/water interface and hydrophobic interactions in the case of the octadecyl alkane) exhibit decreased binding affinities toward OTC, as shown by the low SHG E-fields observed when those surfaces are in contact with OTC. Additionally, it is possible that only the carbonyl group is responsible for the strong interactions of OTC with the carboxylic acid and methyl ester surfaces. Future experiments will investigate the effect of the carbon chain length on OTC interaction with the functionalized adlayers to assess the importance of the nonpolar organic chain in OTC binding for this system.

As shown in Figure 4A, the interaction of OTC with all three surfaces is weak or negligible at pH 2, 5, and 10. However, binding is efficient at pH 8 (binding at pH values between 7.8 and 8.2 also occurred). This result suggests that OTC binds most effectively when in the monoanion form, as shown by the speciation plot in Figure 4B. The highest relative surface coverage, which from adsorption isotherms (vide infra) corresponds to monolayer coverage, occurs again for the methyl ester- and carboxylic acid-functionalized fused quartz/water interfaces. The data shown in Figure 4A indicate again that the combination of polar and nonpolar functional groups enhances OTC binding and is consistent with the adsorption/desorption traces recorded at pH 8 (Figure 3). The SHG E-field enhancement for the polar organic groups may also be due to orientational effects of surface-bound OTC.[48] In the present experiments, we probe using p-polarized fundamental light fields and integrate over all SHG E-field polarization responses. Preliminary results from polarization-resolved SHG measurements of OTC interacting with silica/water interfaces as well as silica/water interfaces functionalized with acid and ester moieties indicate that the SHG response is insensitive to molecular reorientation at pH 8, and our results will be reported in due course.

The highly pH-dependent OTC−surface interaction is consistent with reports by others that indicate a highly pH dependent affinity of OTC to environmental interfaces.[6,12,33,59] Whereas OTC sorption to clays generally decreases with increasing pH,[12,33,59] our results follow those for OTC interaction with iron oxides, where sorption has been shown to increase up to a pH value of 8.[62,63] For the silica/water interface in the presence or absence of carboxylic acid groups held at low pH, coulomb repulsions between the positively charged surface and the quaternary ammonium moiety of the cationic form of OTC are likely to overcome hydrogen bonding and hydrophobic interactions. Likewise, at high pH, coulomb repulsions between the negatively charged surface and the enolate moieties in the dianionic form of OTC are expected to outweigh hydrogen bonding and hydrophobic interactions. A quantitative understanding of the molecular origin governing the enhanced interactions of OTC with all four different interfaces at pH 8 requires that the interfacial pK_a values of OTC bound to these interfaces be known. Through $\chi^{(3)}$ measurements,[67] it is possible to determine if the bulk solution pK_a values for OTC match those of OTC bound to environmental interfaces, and this is the subject of future work.

Our observation that the interaction of OTC with a variety of polar and nonpolar organic groups at interfaces occurs in a reversible fashion almost exclusively around pH 8, which is close to physiological pH (7.4), is consistent with the low OTC retention observed in animals and humans.[2,33] Furthermore, the low OTC surface coverage at the alkyl-functionalized fused quartz/water interface is consistent with the measured low OTC octanol/water partition coefficient, log K_{OW}, of −1.22[6] and its high solubility in water (1 g/mL, or 2 M).[78] To assess the interaction energetics for OTC binding to the various interfaces under investigation, we recorded a series of adsorption isotherms and analyzed them for their free energy of binding.

C. Adsorption Isotherms. Adsorption isotherms were measured for oxytetracycline binding to the four interfaces by recording the SHG signal as a function of increasing OTC concentration at a given pH. Isotherms were measured at pH 2, 5, 8, and 10. Adsorption isotherms for the four interfaces at pH 8 are shown in Figure 5 with their corresponding Langmuir adsorption model fits.[79] Detailed analyses of the Langmuir adsorption model applied to SHG adsorption isotherms have been published previously.[45,46] A summary of thermodynamic parameters obtained from the isotherms is listed in Table 1. The adsorption free energies range from 36 to 43 kJ/mol, which is consistent with a combination of hydrogen bonding (on the order of 20 kJ/mol) and hydrophobic interactions (2−8 kJ/mol per methylene or methyl group).[79,80] The methyl ester-functionalized fused quartz/water interface exhibits the highest equilibrium binding constant, K_{eq}, of $7(1) \times 10^5$ M^{-1}, as well as the lowest OTC concentration necessary to reach monolayer

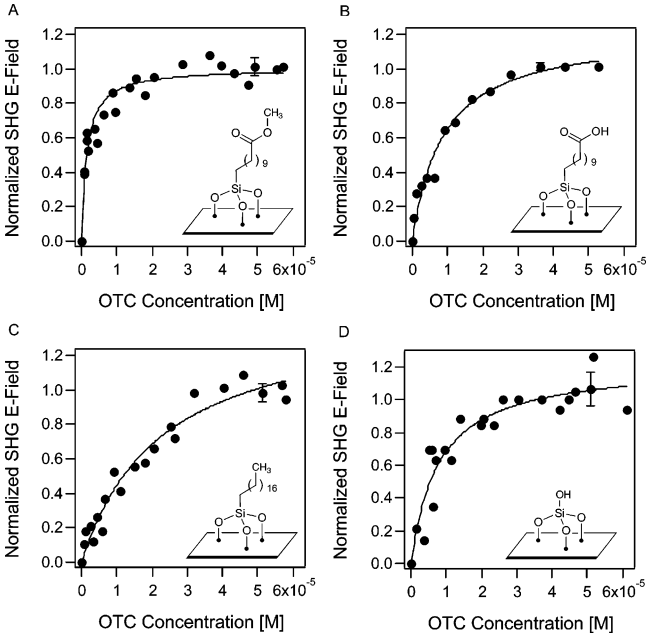

Figure 5. Adsorption isotherms for OTC measured at pH 8 and 300 K for (A) methyl ester-functionalized, (B) carboxylic acid-functionalized, (C) octadecyl alkane-functionalized, and (D) fused quartz/water interfaces. The solid lines are fits of the Langmuir model to the data.

OTC coverage (2.0×10^{-5} M). Although the carboxylic acid- and methyl ester-functionalized fused quartz/water interfaces result in similar OTC surface coverages, as shown in Figure 4A, the onset of monolayer formation occurs at a distinctly lower OTC concentration for the methyl ester surface (see Figure 5A). This suggests that hydrophobic interactions as well as hydrogen-bond acceptor interactions with OTC contribute to the binding of OTC to the methyl ester-functionalized fused quartz/water interfaces.

OTC interaction with the carboxylic acid-functionalized fused quartz/water interface (Figure 5B) may rely more heavily on hydrogen-bond donating interactions, with less-pronounced hydrophobic interactions, as the OTC concentration necessary to reach monolayer OTC surface coverage on the acid-functionalized fused quartz/water interface is similar to that of the plain fused quartz/water interface (Figure 5D). This is consistent with the slightly lower equilibrium binding constants calculated for the carboxylic acid-functionalized fused quartz/water interface and the plain fused quartz/water interface (no organic adlayers present).

Finally, the interaction of OTC with the octadecyl alkane-functionalized fused quartz/water interface (Figure 5C) results in the lowest K_{eq} at pH 8 with a value of $4.4(2) \times 10^4$ M^{-1}. This is expected from the relatively weak binding energy typically associated with hydrophobic interactions among hydrocarbons, which are on the order of 2−8 kJ/mol per CH_2 group.[80,81] Additionally, the octadecyl alkane-functionalized fused quartz/water interface does not appear to reach full monolayer coverage within the concentration regime examined in this work. It is likely that the OTC surface coverage would continue to increase slightly with higher OTC concentrations.

It is interesting to note that the isotherm results for OTC binding to the methyl ester- and carboxylic acid-functionalized fused quartz/water interfaces follow a simple Langmuir adsorption model. In previously published studies of hexavalent chromium binding to these surfaces, the isotherms exhibited a significant curvature in the submonolayer regime, which were modeled with the Frumkin−Fowler−Guggenheim adsorption model.[75,82] This model includes a cooperative effect of lateral adsorbate−adsorbate interactions between the chromate anions adsorbed on the flexible adsorption sites of the organic adlayers. This behavior is not apparent for OTC binding to these surfaces and may be due to multiple binding sites available on the much larger, polyprotic OTC molecule in comparison to the small tetrahedral chromate anion.

4. Environmental Implications

The thermodynamic measurements performed in this study can easily be applied to a commonly used pollutant transport model, the K_d model.[43,83] This model is routinely used by regulatory organizations, including the Environmental Protection Agency, to assess environmental contaminant risks and remediation strategies. The K_d model allows for quantification of how a pollutant interacts with a particular soil environment and is based on the partition coefficient, K_d, which is defined as the ratio of the total equilibrium concentration of sorbed pollutant and the total equilibrium concentration of pollutant in solution.[84] This K_d value can then be incorporated into the expression for the retardation factor, R_f, which provides a measure for how far the pollutant will travel with respect to free-flowing groundwater[43]

$$R_f = 1 + \frac{\rho}{n} K_d \tag{4}$$

where ρ is the bulk density of the soil and n is its porosity (i.e., fraction of total soil volume that is not bulk solid).[43,84] Typical ρ/n values for fused quartz-rich soil environments range from 4 to 10 g/cm^3.[43] We are able to calculate a surface-specific K_d

TABLE 1: Summary of Thermodynamic Binding Parameters Obtained from Langmuir Model Fit for Surfaces Investigated

	fused quartz			methyl ester		
pH	K (M^{-1})	$-\Delta G^o_{ads}$[a] (kJ/mol)	OTC_{mono} (M)	K (M^{-1})	$-\Delta G^o_{ads}$[a] (kJ/mol)	OTC_{mono} (M)
2	[b]			$1.2(9) \times 10^5$	39(1)	1.5×10^{-5}
5						
8	$1.3(5) \times 10^5$	41(1)	3×10^{-5}	$7(1) \times 10^5$	43(1)	2.0×10^{-5}
10				$2.5(5) \times 10^5$	41(1)	1.5×10^{-5}

	carboxylic acid			octadecyl alkane		
pH	K (M^{-1})	$-\Delta G^o_{ads}$[a] (kJ/mol)	OTC_{mono} (M)	K (M^{-1})	$-\Delta G^o_{ads}$[a] (kJ/mol)	OTC_{mono} (M)
2						
5	$4.2(2) \times 10^4$	36(2)	2.5×10^{-5}			
8	$1.1(3) \times 10^5$	41(1)	3.0×10^{-5}	$4.4(2) \times 10^4$	39(1)	$>6 \times 10^{-5}$
10	$2(2) \times 10^5$	40(2)	1.5×10^{-5}			

[a] Free energy values are referenced to the molarity of water under standard conditions (55.5 M). [b] An empty space indicates surface coverages below the detection limit (<10−20% of a monolayer).

TABLE 2: Partition Coefficients and Corresponding Retardation Factor Values for OTC Binding to Surfaces Studied

surface	K_d (ml/g)	R_f
alkyl	0.011	1.04−1.11
fused quartz	0.021	1.08−1.21
carboxylic acid	0.021	1.08−1.21
methyl ester	0.051	1.20−1.51

value for OTC binding to the various interfaces studied using the linear portion of the adsorption isotherm measurements. After converting the OTC surface coverage and bulk concentration units to units of g_{OTC}/g_{quartz} and g/mL,[44] respectively, the slope of the linear submonolayer region results in a K_d value in units of mL/g. The K_d and R_f values for oxytetracycline binding to the four interfaces at pH 8 are listed in Table 2. Because these values are calculated from the adsorption isotherms, it is not surprising that the results mirror those of the thermodynamic parameters. The alkyl surface has the lowest K_d value at 0.011 mL/g ($R_f = 1.04-1.11$), the fused quartz and carboxylic acid surfaces have the same intermediate K_d value of 0.021 mL/g ($R_f = 1.08-1.21$), and the methyl ester surface has the largest K_d value at 0.051 mL/g ($R_f = 1.20-1.51$). This indicates that OTC will be the least mobile in methyl ester-rich soil environments at pH 8, with a relative retardation of 20−50% with respect to groundwater. This is consistent with literature results that show higher K_d values for soils with higher organic carbon content.[33]

The K_d model, however, has significant limitations in its ability to predict pollutant transport in various soils. One of these limitations is rooted in the use of only one general K_d value for a given soil composition. Ternary diagrams, commonly used in geochemical disciplines to depict the relative chemical compositions of rocks and soils, allow us to move beyond this limitation of the K_d model and determine the effective binding constant for a soil due to contributions from up to three types of interactions. The binding constants obtained from our thermodynamic adsorption isotherm experiments indicate that we can group the interactions between OTC and the various surfaces into three classes: (1) hydrogen bond donor and acceptor (HBD/HBA), which include the fused quartz and carboxylic acid surfaces; (2) hydrogen bond acceptor only (HBA), which includes the methyl ester surface; and (3) hydrophobic only (HP) interaction, which includes the alkyl surface.

We can therefore construct a ternary plot that permits calculation of the relative contributions of the chemical functionalities to the equilibrium binding constant for any chemical composition of the organic adlayers under investigation in this work (Figure 6A). The total equilibrium constant, K_{tot}, is obtained from the summation of the contribution from the three interactions as follows

$$K_{tot} = \sum f_i K_{eq,i} \quad (5)$$

Here, f_i is the fraction of chemical constituents interacting with OTC via binding class i. For example, if the soil under question exhibits 30% HBD/HBA behavior, and 40% hydrophobic behavior, then the remaining 30% of the soil must exhibit HBA behavior. At a pH of 8, the relative contributions to the equilibrium binding constant from the three types of interactions for this particular soil composition would result in a K_{tot} of approximately $2.6(1) \times 10^5$ M^{-1} (star in Figure 6A). Cooperative effects are not taken into account in eq 5, but this issue will be addressed in future work that focuses on adlayers with mixed chemical compositions.

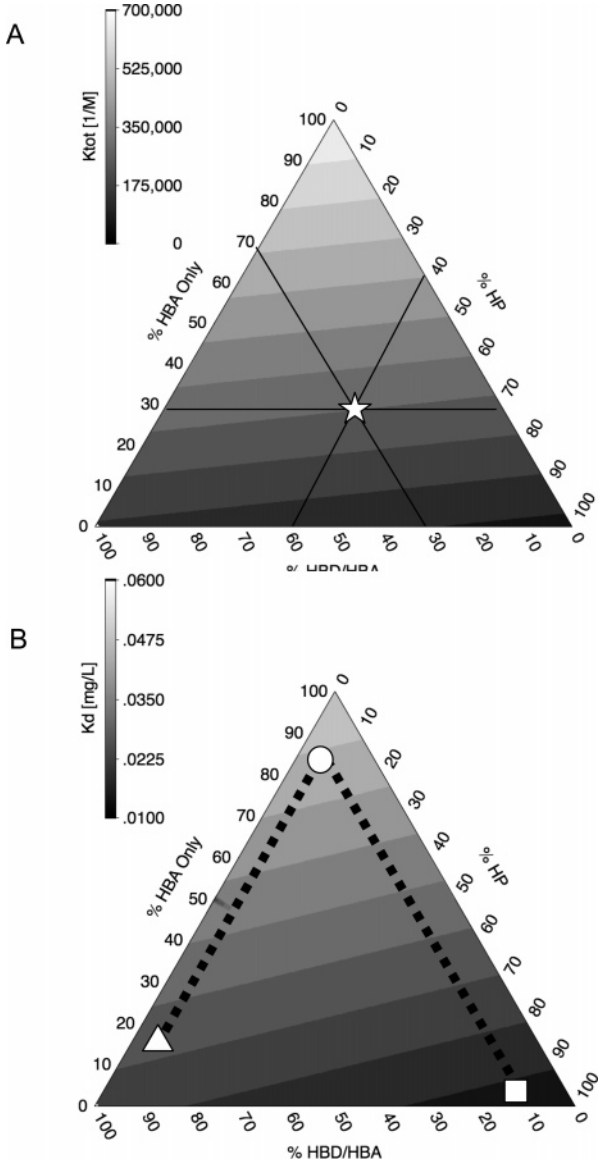

Figure 6. Ternary plots for the three types of interactions involved in OTC binding in this work for (A) the equilibrium binding constant, K_{eq}, where the solid lines are a guide to the eye for determining the K_{tot} for a soil composed of 30% HP, 40% HBD/HBA, and 30% HBA character, and (B) the partition coefficient, K_d, where the dashed line marks the temporal evolution of the degree of oxidation in organic adlayers at the mineral/water interface (square, unoxidized hydrophobic surface; circle, oxidation to ester groups; and triangle, ester conversion to carboxylic acid groups).

At a given pH, different binding events are possible on a soil particle. Using the ternary model, we have the ability to assign individual binding constants to individual classes of adsorption sites. This allows us to map OTC−mineral interactions with spatial resolution, and a specific K_d value can be assigned to a spatial coordinate on a colloid surface. However, if only an average composition of the soil is known, then the surface-specific thermodynamic parameters obtained in these studies can be used to describe the OTC−mineral interactions on a macroscopic scale.

In the development of antibiotic resistance, one must consider the effects of both spatial and temporal exposure of a microbe to an antibiotic. Temporal exposure addresses how long a microbe is in contact with an antibiotic. If the microbe has continuous, long-term contact with the antibiotic, the likelihood of the microbe developing resistance is increased. This can be

a significant issue, as many antibiotics, including OTC, can remain biologically active in soil for weeks to months.[2] In addition, the chemical composition of organic-rich soils is likely to change in oxidizing environments. Figure 6B shows that the K_d parameter calculated for the adsorption isotherm measurements presented in the previous section can increase from approximately 0.01 mL/g (square) in unoxidized hydrophobic portions of natural organic matter to approximately 0.05 mL/g (circle) upon aging. Aging may initially involve ester formation, followed by formation of the carboxylic acid, which would ultimately result in lower K_d values (triangle). It is important to note that this analysis is applicable to the relatively simple systems studied in this work, but will undoubtedly require further modification for application to more complex environmental systems such as clays and iron oxides, which will be the focus of future SHG studies. Clearly, a thorough understanding of antibiotic mobility in soils, and its connection to the degree of oxidation in organic adlayers at mineral/water interfaces, is critical to developing predictive frameworks for the onset of drug-resistance in bacteria. The quantitative thermodynamic data reported in this work represents an important step in that direction.

V. Conclusion

The surface-specific binding behavior of the antibiotic oxytetracycline to environmental interfaces was investigated using second harmonic generation (SHG). This study shows that OTC binding to fused quartz and alkyl-, methyl ester-, and carboxylic acid-functionalized fused quartz interfaces is fully reversible and highly pH dependent. The relative OTC uptake is highest at pH 8 for the organic-functionalized surfaces, and surface saturation occurs at the lowest OTC concentrations for the methyl ester-functionalized fused quartz/water interface. Adsorption isotherms follow a Langmuir adsorption model and indicate that the binding process is dominated by hydrogen bonding and hydrophobic interactions, with free energies of adsorption on the order of 40 kJ/mol for all interfaces studied. The results indicate that OTC transport in the environment will depend heavily on soil pH and composition.

Using the data from our isotherm measurements, we are able to calculate surface-specific partition coefficient values that can easily be incorporated into the K_d model, a commonly used transport model that predicts pollutant mobility in the environment. By modeling our data with a ternary plot, however, we can improve upon the generalities of the K_d model. This type of plot allows us to determine the relative contributions to the OTC binding thermodynamics of three types of interactions and calculate the total equilibrium constant for various soil compositions with these binding characteristics. Insofar as the results from this model study can be expanded to natural environments, this work provides important information on how OTC travels in various soil environments. The quantitative thermodynamic and transport parameters derived from this work link OTC mobility with the development of bacterial antibiotic resistance and can be used to predict how oxytetracycline use in agriculture impacts antibiotic resistance in soil bacteria.

Acknowledgment. A.L.M. gratefully acknowledges support from an EPA Science to Achieve Results Graduate Fellowship. The authors also acknowledge support from an NSF CAREER Grant in Experimental Physical Chemistry and partial support from the Chemical Sciences, Geosciences and Biosciences Division, Office of Basic Energy Sciences, Office of Science, United States Department of Energy. F.M.G. acknowledges a Dow Chemical Company Research Professorship.

References and Notes

(1) D'Costa, V. M.; McGrann, K. M.; Hughes, D. W.; Wright, G. D. *Science* **2006**, *311*, 374.
(2) Halling-Sorensen, B.; Nielsen, S. N.; Lanzky, P. F.; Ingerslev, F.; Lutzhoft, H. C. H.; Jorgensen, S. E. *Chemosphere* **1998**, *36*, 357.
(3) Kay, P.; Blackwell, P. A.; Boxall, A. B. A. *Chemosphere* **2005**, *59*, 951.
(4) Kummerer, K. *J. Antimicrob. Chemother.* **2003**, *52*, 5.
(5) Kummerer, K. *J. Antimicrob. Chemother.* **2004**, *54*, 311.
(6) Tolls, J. *Environ. Sci. Technol.* **2001**, *35*, 3397.
(7) Barnes, K. K.; Kolpin, D. W.; Meyer, M. T.; Thurman, E. M.; Furlong, E. T.; Zaugg, S. D.; Barber, L. B. *Water-Quality Data for Pharmaceuticals, Hormones, and Other Organic Wastewater Contaminants in U. S. Streams, 1999−2000*; U. S. Geological Survey Open-File Report 02-94; U. S. Geological Survey: Reston, VA, 2002.
(8) Giger, W.; Alder, A. C.; Golet, E. M.; Kohler, H. P. E.; McArdell, C. S.; Molnar, E.; Siegrist, H.; Suter, M. J. F. *Chimia* **2003**, *57*, 485.
(9) Goni-Urriza, M.; Capdepuy, M.; Arpin, C.; Raymond, N.; Caumette, P.; Quentin, C. *Appl. Environ. Microbiol.* **2000**, *66*, 125.
(10) Jones, A. D.; Bruland, G. L.; Agrawal, S. G.; Vasudevan, D. *Environ. Toxicol. Chem.* **2005**, *24*, 761.
(11) Simon, N. S. *Environ. Sci. Technol.* **2005**, *39*, 3480.
(12) Kulshrestha, P.; Giese, R. F.; Aga, D. S. *Environ. Sci. Technol.* **2004**, *38*, 4097.
(13) Schwab, B. W.; Hayes, E. P.; Fiori, J. M.; Mastrocco, F. J.; Roden, N. M.; Cragin, D.; Meyerhoff, R. D.; D'Aco, V. J.; Anderson, P. D. *Regul. Toxicol. Pharmacol.* **2005**, *42*, 296.
(14) Blackwell, P. A.; Boxall, A. B. A.; Kay, P.; Noble, H. *J. Agric. Food Chem.* **2005**, *53*, 2192.
(15) Pedersen, J. A.; Soliman, M.; Suffet, I. H. *J. Agric. Food Chem.* **2005**, *53*, 1625.
(16) Yang, S. W.; Carlson, K. *Water Res.* **2003**, *37*, 4645.
(17) Delepee, R.; Maume, D.; Le Bizec, B.; Pouliquen, H. *J. Chromatogr., B* **2000**, *748*, 369.
(18) Witte, W. *Science* **1998**, *279*, 996.
(19) Ferber, D. *Science* **2003**, *301*, 1027.
(20) Wise, R.; Hart, T.; Cars, O.; Streulens, M.; Helmuth, R.; Huovinen, P.; Sprenger, M. *Br. Med. J.* **1998**, *317*, 609.
(21) Shea, K. M. *Pediatrics* **2004**, *114*, 862.
(22) Ferber, D. *Science* **2000**, *288*, 792.
(23) Ferber, D. *Science* **2002**, *295*, 27.
(24) Austin, D. J.; Kristinsson, K. G.; Anderson, R. M. *Proc. Natl. Acad. Sci. U.S.A.* **1999**, *96*, 1152.
(25) Molbak, K.; Baggesen, D. L.; Aarestrup, F. M.; Ebbesen, J. M.; Engberg, J.; Frydendahl, K.; Gerner-Smidt, P.; Petersen, A. M.; Wegener, H. C. *N. Engl. J. Med.* **1999**, *341*, 1420.
(26) Smith, K. E.; Besser, J. M.; Hedberg, C. W.; Leano, F. T.; Bender, J. B.; Wicklund, J. H.; Johnson, B. P.; Moore, K. A.; Osterholm, M. T. *N. Engl. J. Med.* **1999**, *340*, 1525.
(27) Smith, D. L.; Dushoff, J.; Morris, J. G. *PLoS Med.* **2005**, *2*, 731.
(28) Palumbi, S. R. *Science* **2001**, *293*, 1786.
(29) *Food Safety: The Agricultural Use of Antibiotics and Its Implications for Human Health: Report to the Honorable Tom Harkin, Ranking Minority Member, Committee on Agriculture, Nutrition, and Forestry, U. S. Senate;* Report GAO/RCED-99-74; U.S. Government Accountability Office: Washington, DC, 1999.
(30) *A Public Health Action Plan to Combat Antimicrobial Resistance* Centers for Disease Control and Prevention: Atlanta, GA, 2006; Please see: http://www.cdc.gov/drugresistance/actionplan/index.htm.
(31) Hileman, B. *Chem. Eng. News* **2005**, *83*, 16.
(32) *Overcoming Antimicrobial Resistance*; World Health Organization: Geneva, Switzerland, 2000. Please see http://www.who.int/infectious-disease-report/2000/index.html
(33) Sassman, S. A.; Lee, L. S. *Environ. Sci. Technol.* **2005**, *39*, 7452.
(34) Ferber, D. *Science* **2000**, *288*, 792.
(35) Chee-Sanford, J. C.; Aminov, R. I.; Krapac, I. J.; Garrigues-Jeanjean, N.; Mackie, R. I. *Appl. Environ. Microbiol.* **2001**, *67*, 1494.
(36) Attrassi, B.; Saghi, M.; Flatau, G. *Environ. Technol.* **1993**, *14*, 1179.
(37) Samuelsen, O. B.; Torsvik, V.; Ervik, A. *Sci. Total Environ.* **1992**, *114*, 25.
(38) Rumbaugh, K. P.; Griswold, J. A.; Iglewski, B. H.; Hamood, A. N. *Infect. Immun.* **1999**, *67*, 5854.
(39) Finlay, B. B.; Cossart, P. *Science* **1997**, *276*, 718.
(40) Bruun, M. S.; Schmidt, A. S.; Dalsgaard, I.; Larsen, J. L. *J. Aquat. Anim. Health* **2003**, *15*, 69.
(41) Brown, G. E. *Science* **2001**, *294*, 67.
(42) Evangelou, V. P. *Environmental Soil and Water Chemistry*; John Wiley & Sons: New York, 1998.

(43) Langmuir, D. *Aqueous Environmental Geochemistry*; Prentice-Hall: New Jersey, 1997.
(44) Mifflin, A. L.; Gerth, K. A.; Geiger, F. M. *J. Phys. Chem. A* **2003**, *107*, 9620.
(45) Mifflin, A. L.; Gerth, K. A.; Weiss, B. M.; Geiger, F. M. *J. Phys. Chem. A* **2003**, *107*, 6212.
(46) Al-Abadleh, H. A.; Mifflin, A. L.; Bertin, P. A.; Nguyen, S. T.; Geiger, F. M. *J. Phys. Chem. B* **2005**, *109*, 9691.
(47) Al-Abadleh, H. A.; Mifflin, A. L.; Musorrafiti, M. J.; Geiger, F. M. *J. Phys. Chem. B* **2005**, *109*, 16852.
(48) Konek, C. T.; Illg, K. D.; Al-Abadleh, H. A.; Voges, A. B.; Yin, G.; Musorrafiti, M. J.; Schmidt, C. M.; Geiger, F. M. *J. Am. Chem. Soc.* **2005**, *127*, 15771.
(49) Al-Abadleh, H. A.; Voges, A. B.; Bertin, P. A.; Nguyen, S. T.; Geiger, F. M. *J. Am. Chem. Soc.* **2004**, *126*, 11126.
(50) Greenwald, R. A.; Hillen, W.; Nelson, M. L. *Tetracyclines in Biology, Chemistry and Medicine*; Birkhauser Verlag: Boston, 2001.
(51) Hochstein, F. A.; Stephens, C. R.; Conover, L. H.; Regna, P. P.; Pasternack, R.; Brunings, K. J.; Woodward, R. B. *J. Am. Chem. Soc.* **1952**, *74*, 3708.
(52) Conover, L. H.; Moreland, W. T.; English, A. R.; Stephens, C. R.; Pilgrim, F. J. *J. Am. Chem. Soc.* **1953**, *75*, 4622.
(53) Stephens, C. R.; Conover, L. H.; Hochstein, F. A.; Regna, P. P.; Pilgrim, F. J.; Brunings, K. J.; Woodward, R. B. *J. Am. Chem. Soc.* **1952**, *74*, 4976.
(54) Chopra, I.; Roberts, M. *Microbiol. Mol. Biol. Rev.* **2001**, *65*, 232.
(55) Boxall, A. B. A. *EMBO Rep.* **2004**, *5*, 1110.
(56) Corey, R. R.; Byrnes, J. M. *Appl. Microbiol.* **1963**, *11*, 481.
(57) Lien, H. T.; Long, H. T.; Ha, N. T. T.; Lam, P. D. *Alliance for the Prudent Use of Antibiotics Newsletter* **1994**, *12*, 4.
(58) Schneider, S.; Schmitt, M. O.; Brehm, G.; Reiher, M.; Matousek, P.; Towrie, M. *Photochem. Photobiol. Sci.* **2003**, *2*, 1107.
(59) Figueroa, R. A.; Leonard, A.; Mackay, A. A. *Environ. Sci. Technol.* **2004**, *38*, 476.
(60) Pinsuwan, S.; Alvarez-Nunez, F. A.; Tabibi, S. E.; Yalkowsky, S. H. *J. Pharm. Sci.* **1999**, *88*, 535.
(61) Hasan, T.; Khan, A. U. *Proc. Natl. Acad. Sci. U.S.A.* **1986**, *83*, 4604.
(62) Gu, C.; Karthikeyan, K. G. *Environ. Sci. Technol.* **2005**, *39*, 2660.
(63) Figueroa, R. A.; Mackay, A. A. *Environ. Sci. Technol.* **2005**, *39*, 6664.
(64) MacKay, A. A.; Canterbury, B. *J. Environ. Qual.* **2005**, *34*, 1964.
(65) Leypold, C. F.; Reiher, M.; Brehm, G.; Schmitt, M. O.; Schneider, S.; Matousek, P.; Towrie, M. *Phys. Chem. Chem. Phys.* **2003**, *5*, 1149.
(66) Schack, C. J. *Inorg. Chem.* **1967**, *6*, 1938.
(67) Eisenthal, K. B. *Chem. Rev.* **1996**, *96*, 1343.
(68) Shen, Y. R. *The Principles of Nonlinear Optics*; John Wiley & Sons: New York, 1984.
(69) Heinz, T. F. *Nonlinear Surface Electromagnetic Phenomena*; Elsevier: New York, 1991.
(70) Zumdahl, S. S.; Zumdahl, S. A. *Chemistry*, 6th ed.; Houghton Mifflin: Boston, 2003.
(71) Beecham, A. F.; Hurley, A. C.; Johnson, C. H. J. *Aust. J. Chem.* **1980**, *33*, 699.
(72) Li, X. S.; Liu, L.; Schlegel, H. B. *J. Am. Chem. Soc.* **2002**, *124*, 9639.
(73) Al Usta, K.; Dosch, H.; Peisl, J. *Z. Phys. B.* **1990**, *79*, 409.
(74) Al-Abadleh, H. A.; Voges, A. B.; Bertin, P. A.; Nguyen, S. T.; Geiger, F. M. *J. Am. Chem. Soc.* **2004**, *126*, 11126.
(75) Al-Abadleh, H. A.; Mifflin, A. L.; Musorrafiti, M. J.; Geiger, F. M. *J. Phys. Chem. B.* **2005**, *109*, 16852.
(76) Kondo, Y.; Matthews, W. A.; Solomon, S.; Koike, M.; Hayashi, M.; Yamazaki, K.; Nakajima, H.; Tsukui, K. *J. Geophys. Res. (Atmos.)* **1994**, *99*, 14535.
(77) Voges, A. B.; Al-Abadleh, H. A.; Musorrafiti, M. J.; Bertin, P. A.; Nguyen, S. T.; Geiger, F. M. *J. Phys. Chem. B* **2004**, *108*, 18675.
(78) *The Merck Index*, 13th ed.; O'Neil, M. J., Ed.; Merck Research Laboratories: Whitehouse Station, NJ, 2001.
(79) Atkins, P. W. *Physical Chemistry*, 6th ed.; Oxford University Press: Oxford, U.K., 1998.
(80) Dubois, L. H.; Nuzzo, R. G. *Annu. Rev. Phys. Chem.* **1992**, *43*, 437.
(81) Atkins, P. W. *General Chemistry*; Scientific American Books: New York, 1989.
(82) Al-Abadleh, H. A.; Mifflin, A. L.; Bertin, P. A.; Nguyen, S. T.; Geiger, F. M. *J. Phys. Chem. B* **2005**, *109*, 9691.
(83) *Understanding Variation in Partition Coefficient, Kd, Values: Introduction*; United States Environmental Protection Agency: Washington, DC, 2003; Please see www.epa.gov/radiation/cleanup/partition.htm.
(84) Schwarzenbach, R. P.; Gschwend, P. M.; Imboden, D. M. *Environmental Organic Chemistry*, 2nd ed.; John Wiley and Sons: Hoboken, New Jersey, 2003.